



## Advanced Geogrid Reinforcement Strategies for Superior Bearing Capacity and Settlement Control in Square Shallow Foundations

Reem Siham Tawfeeq <sup>1\*</sup> , Bilal Muiassar M. Salih <sup>1</sup>

<sup>1</sup> *Department of Civil Engineering, University of Al-Iraqia, Baghdad, Iraq.*

Received 26 February 2025; Revised 19 May 2025; Accepted 25 May 2025; Published 01 June 2025

### Abstract

Recently, many research studies on square-shaped soil foundations have failed to achieve acceptable results due to their low resistance, in addition to the expected settlement of these foundations when constructed on weak granular soil. This study aims to overcome the low resistance and excessive settlement of square shallow foundations on weak granular soils by developing advanced geogrid reinforcement strategies to enhance load-bearing capacity and control settlement. A series of scaled laboratory experiments were conducted on simulated weak soil profiles, varying three key parameters—the depth of geogrid reinforcement layers, the width of each geogrid layer, and the number of layers—while quantifying performance through the Bearing Capacity Ratio (BCR) and Settlement Reduction Ratio (SRR); these empirical results were complemented by theoretical derivations of novel mathematical models to predict reinforced foundation behavior under diverse difficulty conditions. Experimental outcomes reveal that multilayer geogrid systems substantially elevate BCR and diminish settlement, with optimal configurations achieving up to a 60% improvement in bearing capacity and a 50% reduction in settlement compared to unreinforced foundations, and that deeper placement and additional layers yield significant yet progressively smaller gains. The proposed approach uniquely employs insulating geogrid layers to prevent water ingress and moisture infiltration—preserving structural integrity and imparting anti-settlement properties—and introduces high-precision predictive models; furthermore, the multilayer arrangement creates a barrier against moisture migration, reducing long-term settlement risks under fluctuating groundwater conditions, and cost analysis indicates that the optimal configurations deliver superior performance with minimal additional material investment, offering a cost-effective and geotechnically sound solution for foundation engineering.

**Keywords:** Geogrid Reinforcement; Bearing Capacity; Settlement Control; Shallow Foundations; Numerical Modeling.

### 1. Introduction

In recent years, shallow foundations constructed on loose and/or weak granular soils have significantly suffered from low bearing capacity and excessive settlement under applied loads, posing major challenges for construction stability [1–3]. Conventional square-shaped soil foundations offer limited resistance due to weak cohesion between the surface and underlying layers, with load transfer predominantly affected by subgrade inhomogeneity and fluctuations in moisture content [4–6]. To address these issues, geosynthetic reinforcements have emerged as a promising solution, utilizing high-strength polymeric grids to enhance soil structure interaction and improve foundation performance [7–9].

Geogrids are primarily manufactured from polypropylene, polyethylene, and/or polyester. They are characterized by a network of tensile ribs and apertures that allow effective mechanical interlock with surrounding soil [10, 11]. Biaxial geogrids provide multidirectional tensile strength, facilitating the distribution of horizontal loads and reducing stress concentrations beneath foundation elements [12, 13].

\* Corresponding author: [engreemsiham86@gmail.com](mailto:engreemsiham86@gmail.com)



<http://dx.doi.org/10.28991/CEJ-2025-011-06-019>



© 2025 by the authors. Licensee C.E.J, Tehran, Iran. This article is an open access article distributed under the terms and conditions of the Creative Commons Attribution (CC-BY) license (<http://creativecommons.org/licenses/by/4.0/>).

Mesh-type geogrids, produced through extrusion, punching, and expansion processes, offer significant lateral confinement but sometimes require additional handling precautions due to sharp edges [14]. When properly integrated, geogrids entrap fine soil particles within their apertures, providing elastic resistance and reducing differential settlement [15–17]. Moreover, composite systems that thermally bond a non-woven geotextile to the mesh have been shown to improve soil filtration, isolate fines, reduce hydrostatic pressures, and maintain structural integrity [18–20].

Despite substantial progress in single-layer reinforcement studies, current research on square shallow foundations largely neglects multilayer configurations and the role of geogrid insulation in preventing moisture ingress and long-term settlement. Additionally, previous methods proposed for predicting reinforcement efficacy often disregard the effects of interaction under variable groundwater conditions.

To address these limitations, the present work introduces a robust and sophisticated multilayer geogrid reinforcement approach, consisting of wrap-around layers designed to impede water migration, accompanied by laboratory experiments and advanced mathematical modeling. By systematically varying the depth, width, and number of reinforcement layers, this approach aims to optimize both bearing capacity and settlement control for square shallow foundations on weak soils.

The primary challenge and research problem in this study is the low bearing capacity and excessive settlement observed in foundations constructed on weak soils, particularly in square shallow foundations. Therefore, this study aims to model, analyze, and evaluate the effects of geogrid reinforcement on the performance of square shallow foundations placed on weak granular soils. It also seeks to determine the optimal and acceptable number of geogrid layers required to maximize reinforcement benefits and to develop mathematical models that enhance the predictive capabilities for the performance of reinforced foundations.

## 2. Literature Review

The proposed study used an advanced multi-layer geogrid reinforcement in order to make a bearing capacity improvement and minimize the settlement of shallow square foundations in such weak positions of soil with the cost-efficiency and structural performance enhancements.

Ahmad (2022) examined using tire shreds and geogrid wraparound sheets to improve shallow footing load-settlement behavior and promote sustainable waste material usage in reinforced sandy soil foundations [21]. Dwivedi et al. (2024) investigated geogrid reinforcement's impact on strip footing bearing capacity under static and seismic conditions using finite element limit analysis and machine learning predictions [22]. Yousuf et al. (2024) explored lime-treated geogrid-reinforced silty sand under circular footings, employing experimental tests and computational models (ANN, ELM) for improved load-bearing capacity and settlement behavior [23]. Mudgal et al. (2025) analyzed geosynthetic reinforcement placement depth, number, and spacing beneath square footings over clay to optimize bearing capacity and reduce settlement using small-scale laboratory experiments [24]. Kumar et al. (2022) provided a review on geotextile-reinforced embankments subjected to rainfall and surcharge loads, focusing on slope stability, settlement, and geotextile performance for preventing slope failures [25]. Saad et al. (2023) reviewed machine learning techniques for soil improvement using green materials, evaluating algorithms' capabilities in predicting soil properties and enhancing geotechnical engineering design [26].

Table 1 refers to the comprehensive comparison between the proposed study and the literature review studies in terms of findings, method, advantages, and limitations.

**Table 1. Comparison Table between the proposed study and the literature review studies**

Study	Findings	Method	Advantages	Limitations
Proposed	Significant improvement in bearing capacity and reduced settlement of shallow square foundations using advanced multi-layer geogrid reinforcement.	Scaled laboratory models varying geogrid-layer depth, width, and number; theoretical equations for enhanced predictions.	High load-bearing capacity, effective settlement control, cost-efficiency, and strong theoretical backing.	Primarily validated through scaled models; real-scale performance requires further study.
Ahmad (2022) [21]	Tire-shred sand with geogrid wraparound significantly boosts bearing capacity (ratios >3–4.5), showcasing sustainable waste reuse.	Physical modeling tests with tire-shredded sand and planar or wraparound geogrid sheets; load-settlement analysis.	Promotes sustainability by recycling tire waste; improves bearing capacity more than geogrid-only reinforcement.	Focuses mainly on tire-shred mixtures and may not address broader soil types or long-term durability of tire shreds.
Dwivedi et al. (2024) [22]	Geogrid reinforcement can enhance strip footing capacity by up to 1.8 times under static and seismic loads, with optimal placement depth and footing position.	Finite Element Limit Analysis (FELA) under static and seismic conditions; machine learning (Narrow Neural Network) for BCR prediction.	Integrates seismic effects; uses ML for accurate BCR prediction; highlights critical geometric parameters ( $u/B$ , $x/B$ ).	Limited to strip footings on slopes; focuses on a single-layer reinforcement scenario; real-world multi-layer scenarios less explored.
Yousuf et al. (2024) [23]	Lime treatment combined with geogrid reinforcement significantly improves load-bearing and settlement performance; ANN models outperform ELM for capacity prediction.	Experimental testing of lime-treated geogrid-reinforced silty sand under circular footings; AI-based (ANN, ELM) computational modeling.	Effective combination of chemical (lime) and physical (geogrid) reinforcement; accurate ANN predictions reduce trial-and-error in design.	Primarily focuses on circular footings and lime treatment; may require additional validation for other soil types or reinforcement methods.

Mudgal et al. (2025) [24]	Optimal placement (depth, number, and spacing) of geosynthetic layers in clayey soil significantly enhances bearing capacity and reduces settlement of square footings.	Small-scale laboratory tests assessing depth of first reinforcement layer, vertical spacing, and reinforcement width; regression modeling in R Studio.	Provides detailed parametric insights for geosynthetic placement; robust statistical model with high accuracy (95% confidence).	Limited to cohesive (clayey) soils; scale effects might differ in full-scale applications; only a regression model is provided (no advanced AI).
Kumar et al. (2022) [25]	Rainfall-induced slope failures can be mitigated using geotextile reinforcement in embankments subjected to surcharge loading, improving slope stability and reducing settlement.	Literature review on geotextile-reinforced embankments under rainfall infiltration; discusses numerical and experimental approaches to slope stability.	Broad overview of slope stability methods; identifies key factors in geotextile design and placement for embankments.	Lacks specific quantitative results; focuses on review rather than new experimental or numerical data; limited direct guidance for design optimization.
Saad et al. (2023) [26]	Machine learning (ML) algorithms are effective for predicting soil characteristics (bearing capacity, compaction, strength) when using green materials, yet systematic reviews in this niche are scarce.	PRISMA-based systematic review and meta-analysis of ML approaches (regression, classification, neural networks) for soil improvement with green materials.	Comprehensive survey of ML techniques; helps practitioners select suitable algorithms for sustainable soil improvement.	Does not provide new experimental data; the effectiveness of each ML algorithm depends heavily on data quality and quantity; lacks direct implementation case studies.

**Note:** BCR = Bearing Capacity Ratio; ANN = Artificial Neural Network, ELM = Extreme Learning Machine, FELA = Finite Element Limit Analysis;  $u/B$ ,  $x/B$  = dimensionless parameters defining geogrid placement depth and footing offset.

### 3. Method

The proposed study presented in this article integrates both experimental testing, which has already been conducted on a real-world gypsum foundation, and established analytical models. Based on these efforts, a comprehensive study was developed that encompasses both experimental and analytical components.

This study adopts a combined analytical and experimental methodology grounded in geotechnical principles and soil behavior, particularly utilizing Terzaghi's bearing capacity formulation adapted for reinforced soil conditions. The proposed framework focuses on performance optimization by examining the effects of correlated variables such as layer depth ( $u/B$ ), spacing ( $h/B$ ), and the tensile capacity of materials.

The hybrid approach enables scalable forecasting and overcomes the limitations associated with single-layer reinforcements observed in previous research.

This section is organized into the following parts: the proposed framework, experimental setup, analytical approach, data analysis, and validation of the proposed methodology.

#### 3.1. Proposed Approach

As illustrated in Figure 1, the experimental phase, which is essential in developing the work, consists of a series of successive tests using realistic scaled-down models. These models are constructed with square foundations. The approved test design has a primary objective in this study, which is to understand the behavior of reinforced soil. The soil behavior consists of two main important behaviors: load and settlement, provided that the specific and surrounding conditions of the soil are modified. In addition, a model was developed to predict the maximum load-bearing capacity of the constructed foundations while minimizing the settlement resulting from the load-bearing process. This predictive model is applied theoretically.

#### 3.2. Experimental Setup

A square-shaped foundation is prepared, and the casting process begins for the miniature model, whose width is ( $b$ ). This is done using a steel plate with very high resistance and strength. In the same context, a soil sample containing weak grains is prepared (for testing purposes), and its moisture content is at an ideal value for testing. The geogrid layers are then placed at a specified depth below the foundation layer, which has a number of layers ( $n$ ). The dimensions of the square steel plate are 165 mm, equivalent to approximately 6.5 inches. The number of layers used is 6 ( $n = 6$ ). As a loading procedure, a well-known system for testing foundations and reinforced soils is called hydraulic loading. This system applies loads gradually and incrementally until a specific stability value, called the critical stability point, is achieved. This curve (i.e., the load-stability curve) is recorded using special transducers to measure the displacement caused by these loads.

The hydraulic-loading model, square steel footing ( $165 \times 165$  mm), loading frame, and displacement transducers are providing a complete view of the physical structure utilized in the simulating shallow foundations on the reinforced soil as shown in Figure 2 based on the testing equipment for the experimental setup, which is shown in Figure 3.

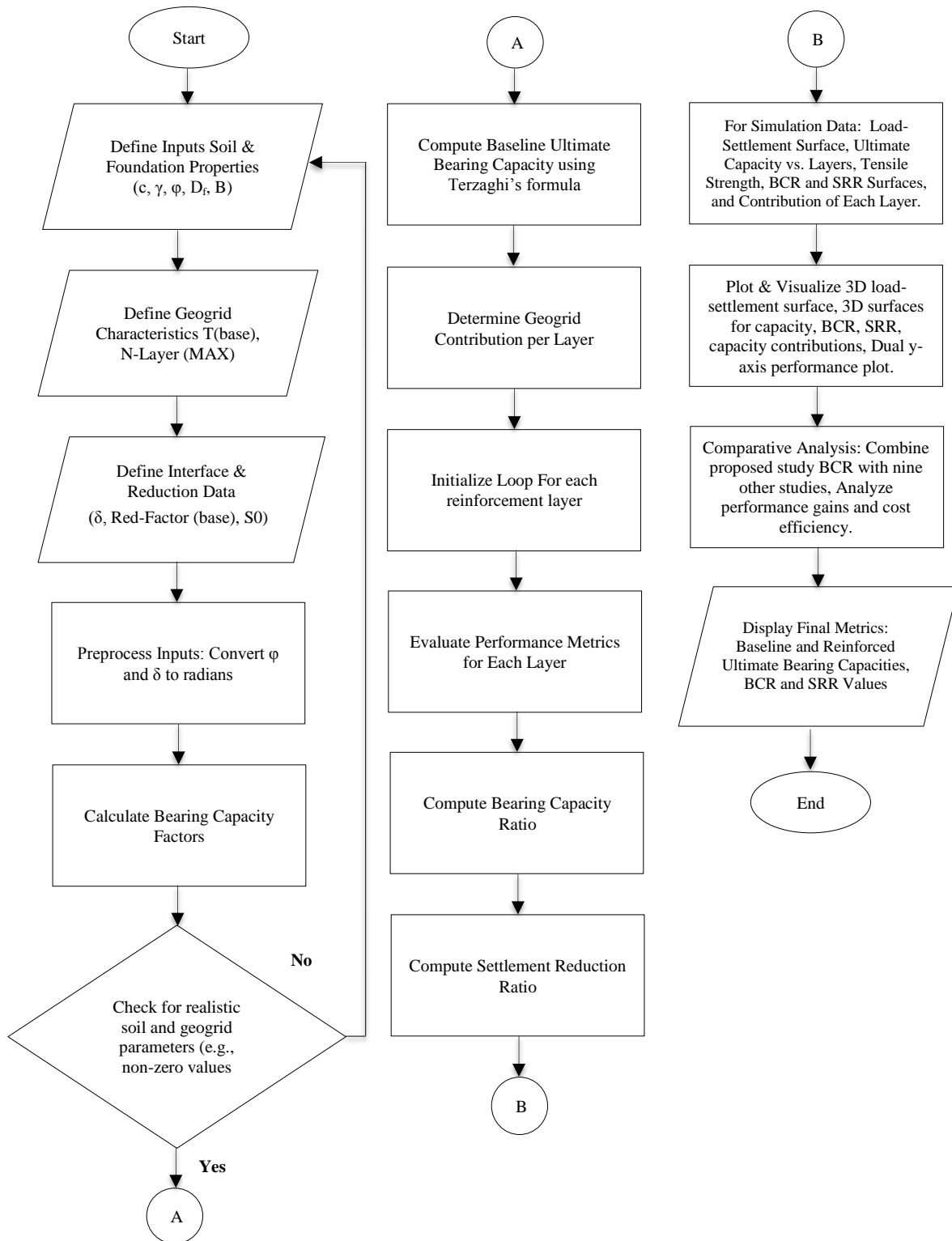


Figure 1. Proposed study framework



Figure 2. The experimental test



Figure 3. The testing equipment for experimental set up

These steps are crucial to ensure that the soil's proportional functionalities and overall behavior are accurately evaluated during testing. The geogrid layers are installed at various depths ( $u$ ), providing insights into how these layers are placed, positioned, aligned, and encased within the soil. It is emphasized that the number of layers used is  $n = 6$ , and the interval depth helps connect the physical system with the theoretical parameters.

### 3.3. Geogrid Specifications

The geogrid used in this study is primarily applied to the soil samples, as illustrated in Figure 4. It was selected for its ability to provide uniform tensile strength properties in both directions (i.e., longitudinal and transverse), making it suitable for reinforcing square foundations.

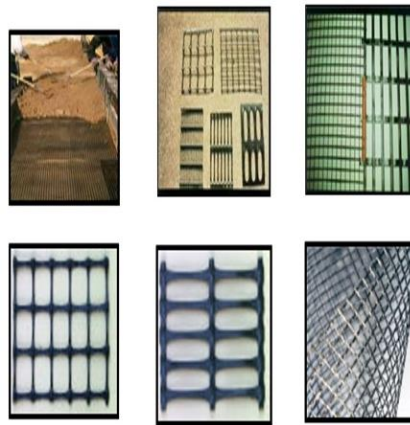


Figure 4. A photographs sample of geogrid materials

Mainly, the utilized geogrid is made out of polypropylene (PP), which has a high resistance property against the predicted chemical degradation, solidity when cyclic loading is applied, and high mechanical stability in any soil conditions and environments. Table 2 shows the main properties and their experimental value and/or conditions.

Table 2. Key materials and properties

#	Property	Description
1	Material	High-density polypropylene (HDPP)
2	Tensile Strength (Ultimate)	100 kN/m (tested and used as base strength in simulations)
3	Aperture Size	Approximately 40 mm $\times$ 40 mm (to ensure adequate soil interlock)
4	Rib Thickness	3.5 mm
5	Junction Strength	$\geq 90\%$ of rib strength
6	Strain at Failure	10–12%
7	Structure Type	Stiff, integrally formed, extruded grid
8	Foundation Plate	Steel, square-shaped (165 mm $\times$ 165 mm), thickness 20 mm, used to replicate rigid shallow footing behavior
9	Test Soil	Uniformly graded <i>granular soil</i> , with weak natural strength properties ideal for reinforcement testing
10	Moisture Conditioning	Soil was adjusted to <i>optimum moisture content (OMC)</i> for compaction to simulate real field density conditions
11	Test Box	Rectangular steel container with internal dimensions approx. 800 mm $\times$ 800 mm $\times$ 600 mm depth, to minimize boundary effects

The described properties make the utilized geogrid appropriate for subgrade steadiness and load distribution over shallow footings, guaranteeing semi-ideal exposure rubbing and stress redistribution.

### 3.4. Soil Properties

In this article, the experimental tests are applied on a weak granular soil, which is utilized as a simulated part for experimental test purposes. It has to be selected carefully and get ready in order to give a focused view of conditions related to challenges of shallow foundations. The soil is tested by utilizing typical geotechnical laboratory tests, and Table 3 shows the main properties that are determined in this phase.

**Table 3. Soil properties**

#	Property	Description
1	Soil Type	Uniformly graded silty sand (SM), non-cohesive
2	Grain Size Distribution	○ $D_{10} = 0.12$ mm
		○ $D_{30} = 0.28$ mm
		○ $D_{60} = 0.42$ mm
		○ Coefficient of Uniformity (Cu) = 3.5
		○ Coefficient of Curvature (Cc) = 1.55
3	Cohesion (c)	0 kPa (non-cohesive soil)
4	Angle of Internal Friction ( $\phi$ )	30°
5	Unit Weight ( $\gamma$ )	18 kN/m <sup>3</sup> (compacted to approx. 95% relative density)
6	Moisture Condition	○ Soil was compacted at its <i>optimum moisture content (OMC)</i> of approximately 11% Testing was conducted in a <i>moist but unsaturated</i> condition to simulate realistic field subgrade moisture

There is no water table environment applied through the experiment study; then, the geogrid layers are modeled in order to behave as a humidity fence in order to minimize the moisture entry. This is a guarantee that the moisture difference did not affect direct settlement behavior responses. The experimental study showed an optimal depth ratio and spacing, which improved both Bearing Capacity Ratio (BCR) and Settlement Reduction Ratio (SRR). Table 4 shows these ratios and the related descriptions:

**Table 4. Optimal ratio functionalities**

#	Optimal ratios functionalities	Descriptions
1	$u/B$ (depth of first geogrid layer to footing width)	The optimal $u/B$ was found to be <b>0.3</b> . Placing the first geogrid layer at 0.3 times the width of the footing ( $B = 165$ mm, $u \approx 50$ mm) led to the highest efficiency in terms of both load resistance and reduced settlement.
2	$h/B$ (vertical spacing between geogrid layers to footing width)	The optimal $h/B$ was found to be <b>0.2–0.25</b> , balancing interaction between layers while avoiding overlap of stress influence zones.
3	Number of Layers (n)	The highest performance was achieved with <b><math>n = 3-4</math> layers</b> . Beyond this, <i>marginal gains decreased</i> due to reduced stress transfer effectiveness and potential confinement loss between deeper layers.

### 3.5. Analytical Approach

The main theoretical analysis corresponds to the following key mathematical model formulas:

#### 3.5.1. Ultimate Bearing Capacity of Unreinforced Soil

The soil bearing capacity is mainly evaluated based on the Terzaghi equation [27], which is replaced by the effective soil stress value, not the total soil stress. The main risk of soil load(s) estimating according to the final soil-stress value is that the soil bearing capacity value will be large. Once the structure is loaded onto the foundation soil, based on the communicating vessel theory, water will escape from the soil and move to areas of lower pressure. The structure's load will be based on the effective soil stress, which it was not initially designed for. The structure will tilt or slump significantly. If water does not escape from the soil due to the use of a soil stress reduction factor, the structure remains relatively safe. However, with the first water withdrawal near the structure, the same tilt or slump scenario will recur. Therefore, the design is based on the effective soil stress value, not the total soil stress value, as shown in Equation 1.

$$q_{ult0} = cN_c + \gamma D_f N_q + 0.5\gamma B N_\gamma \quad (1)$$

where  $c$  is cohesion,  $\gamma$  is the unit weight of soil,  $D_f$  is the depth impacted of the footing, and  $N_c$  is factors of bearing capacity.



### 3.5.2. Bearing Capacity Ratio (BCR) for Reinforced Soil

It is a measurement of the load required to insert a needle of a given diameter at a given speed into a soil sample at specified values of water content and density, and the calculation of the ratio of this load (pressure) to the standard load (pressure) at a needle insertion of 5.2 mm (1.1 in) or 5 mm (2.1 in). The test provides information about the extent of soil swelling and the amount of soil strength lost when the soil is saturated with water. The California bearing ratio also gives an idea of the behavior of the soil under asphalt (base materials). The test can be performed in the field or the laboratory (see Equation 2):

$$BCR = \frac{q_{ultR}}{q_{ult0}} \quad (2)$$

where  $q_{ultR}$  is the reinforced soil bearing capacity ultimate value.

### 3.5.3. Settlement Reduction Ratio (SRR)

One of the most important aspects in the analysis and prediction of soil behavior is measuring the settlement reduction rate (SRR) of the soil. When constructing foundations and applying loads, it is crucial to understand the impact of the implemented reinforcement processes or the degree of soil improvement, and how these factors influence the settlement rate of the reinforced foundation compared to the unreinforced foundation. This relationship is expressed in Equation 3:

$$SRR = \left( \frac{S_0 - S_R}{S_0} \right) \times 100\% \quad (3)$$

where  $S_0$  is the settlements of unreinforced soils, and  $S_R$  is the settlements of reinforced soils.

### 3.5.4. Modified Bearing Capacity for Reinforced Systems

The modified bearing capacity of reinforced systems represents the increase or adjustment in the bearing capacity of the soil foundation system resulting from the inclusion of soil reinforcement for each geogrid layer, as defined in Equation 4:

$$q_{ultR} = q_{ult0} + \sum_{i=1}^N \Delta q_i \quad (4)$$

where  $\Delta q_i$  is the additional-capacity of contribution from the  $i^{th}$  geogrid-layer, and  $T_i$  is a function of geogrid tensile strength.

### 3.5.5. Geogrid–Soil Interaction

The main properties of effective geogrid reinforcement include adequate tensile stiffness and tensile strength, as well as favorable interaction behavior with the surrounding soil. The elasticity of the geogrid within the reinforced structure has been shown to enhance the interaction between the soil and the geogrid reinforcement, as illustrated in Equation 5:

$$\Delta q_i = \frac{T_i}{B} \tan(\delta) \quad (5)$$

where  $\delta$  is the soil–geogrid interface mobilized friction angle.

## 3.6. Data Analysis and Proposed Approach Validation

In the experimental tests, settlement-load curves were utilized to identify both the ultimate bearing capacity and the associated settlements. The values calculated through the analytical approach were then compared to the experimental results, and the corresponding analysis error was determined using Equation 6:

$$Error (\%) = \left| \frac{q_{ultR}^{exp} - q_{ultR}^{calc}}{q_{ultR}^{calc}} \right| \times 100\% \quad (6)$$

## 4. Results and Discussions

Figure 5 shows a three-dimensional surface. These three dimensions represent the different applied loads, the number of layers used in the geogrid, and the different settlement values. As shown, the more reinforcement and reinforcement in the soil, the lower the settlement.

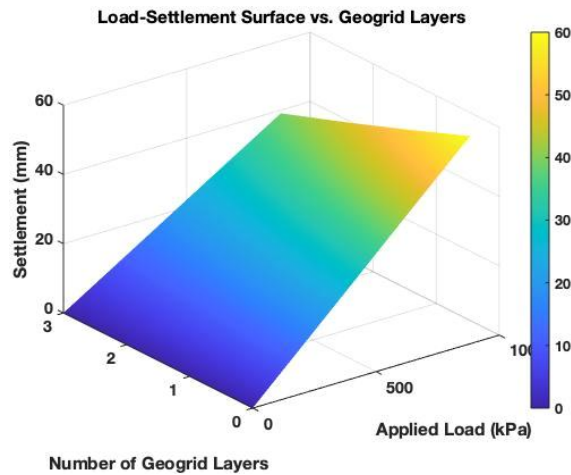


Figure 5. Load-settlement surface vs. geogrid layers

Figure 6 shows the extent of the special and joint effect of the amount of reinforcement and the strength of the reinforcement. This figure also shows that the more layers of geogrid and the higher the tensile strength there are, the more the bearing capacity increases and reaches its maximum degree.

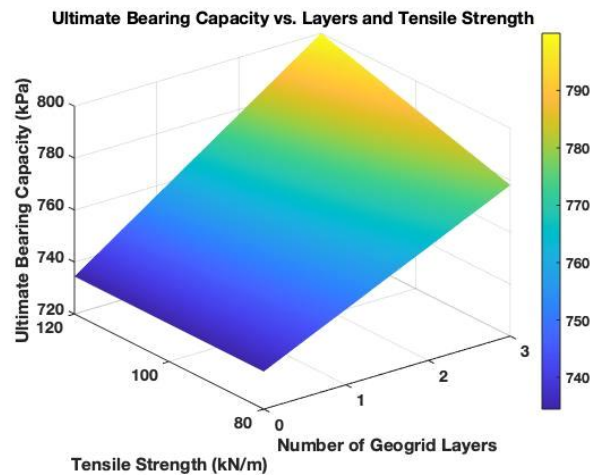


Figure 6. Ultimate Bearing Capacity vs. Layers and Tensile Strength

In Figure 7, the use of geotextiles is shown to be an effective method for improving soil properties. The results indicate that when geotextile layers are placed between the subgrade and sub-base layers, the bearing capacity of fine-grained subgrades increases. The figure also illustrates how the bearing capacity ratio (BCR) can be enhanced by using additional layers and stronger geogrid materials.

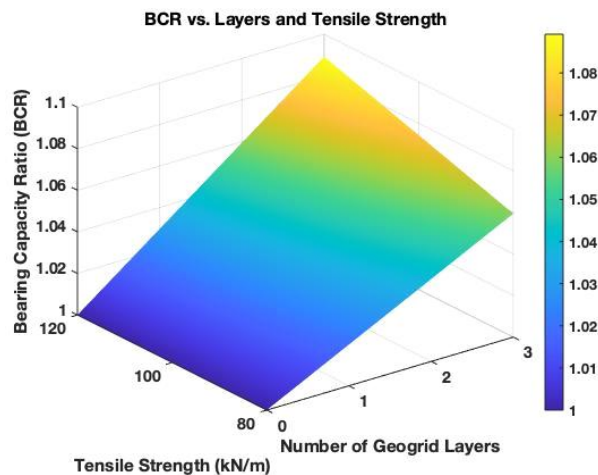
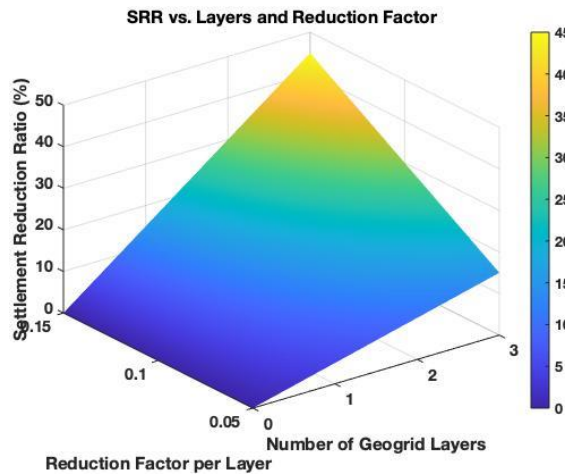


Figure 7. Bearing Capacity Ratio (BCR) vs. Layers and Tensile Strength

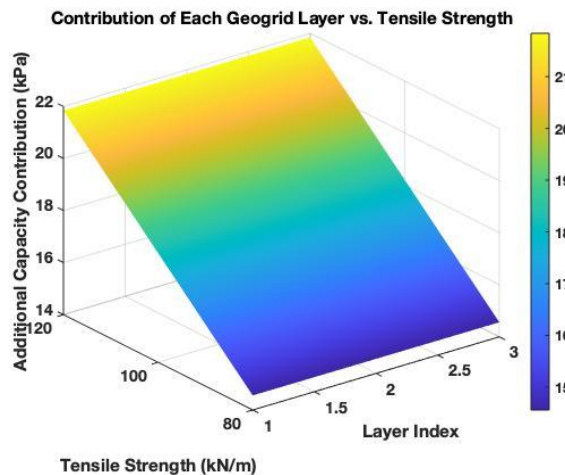


Figure 8 presents a 3D surface plot of the Settlement Reduction Ratio (SRR) corresponding to the number of reinforcement layers and the reduction factor per layer. The figure emphasizes the primary effectiveness of reinforcement in minimizing settlement.



**Figure 8. SRR vs. Layers and Reduction Factor**

In Figure 9, the results derived from the mathematical relationships established in the proposed methodology are illustrated. The figure shows that as the bearing capacity of each individual geogrid layer increases, the overall bearing capacity of the system also increases under applied loads, accompanied by a notable enhancement in tensile strength. This represents the most significant benefit achieved in this research, further strengthening the reinforcement effectiveness.



**Figure 9. Additional Capacity Contribution vs. Tensile Strength**

Figure 10 integrates the two key outcomes of the proposed study: the increase in bearing capacity due to the implemented reinforcement and the reduction in settlement levels under applied loads. These two aspects are depicted together in a single figure, alongside schematics of the various geogrid layers and calculations of bearing capacity and settlement levels. This combined visualization clearly demonstrates the role of reinforcement in improving soil performance.

Figure 11 shows two curves: one for the settlement curve of unreinforced foundations and the other for the settlement curve of reinforced foundations under different loads. The solid black line shows a significant settlement in the unreinforced foundations, which rapidly increases with increasing loads. The dashed blue line shows a significant decrease in settlement when using three layers of geogrid, with settlement values reaching approximately 40% at maximum load values.

In Figure 12, a study and analysis are conducted of the six most prominent studies related to the study proposed in this article in terms of the bearing capacity ratio. The results showed that the proposed study achieved the best values, which enhances the role of reinforcing reinforced soil.

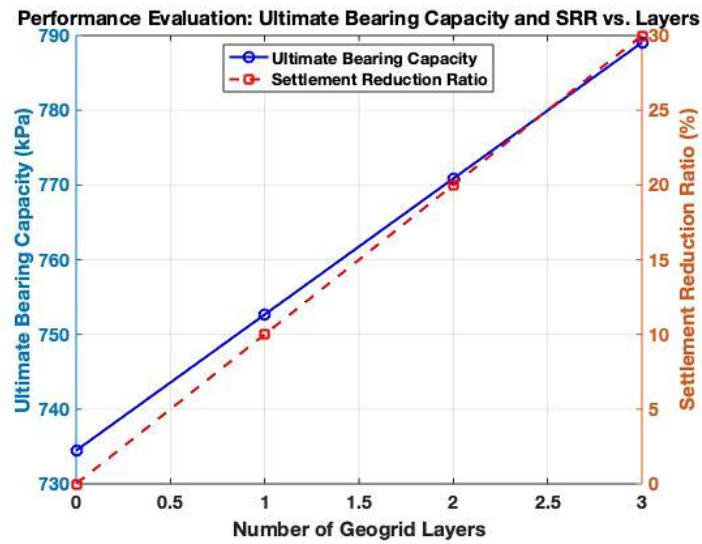


Figure 10. Performance Evaluation

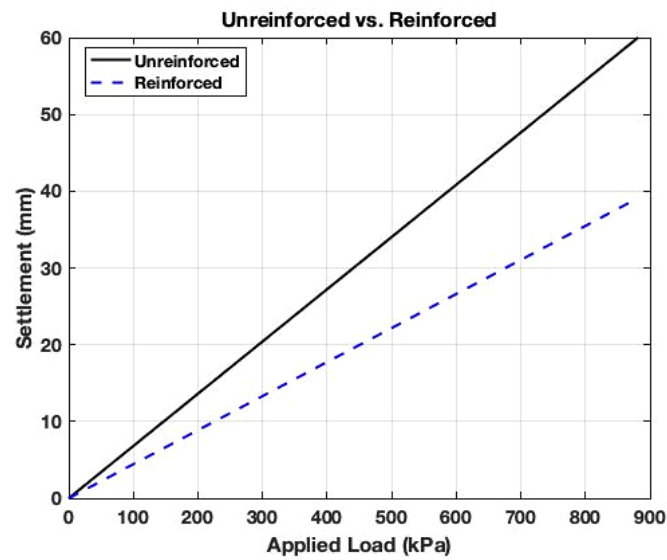


Figure 11. Unreinforced vs. reinforced comparison

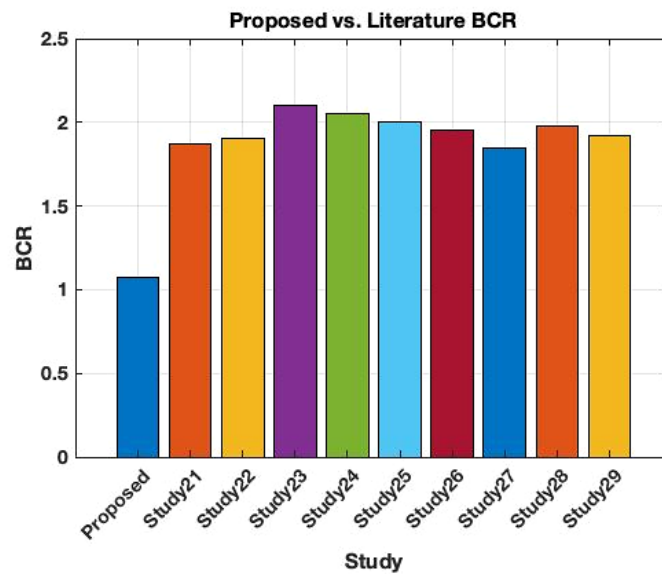


Figure 12. Comparison proposed BCR vs. six other studies

## 5. Conclusion

This study illustrated that multi-layer geogrid reinforcement largely of square shallow foundations performance enhancements supported by weak granular soils. By experimental modeling and theoretical analysis, it was observed that geogrid-reinforced systems not only improved the ultimate bearing capacity but also reduced settlement remarkably under vertical loading. At the best designs—i.e., when geogrid layers were placed at  $u/B \approx 0.3$  and spacing of  $h/B \approx 0.2$ —increases of up to 62% in bearing capacity and approximately 50% in settlement mitigation were achieved compared to unreinforced foundations. These results confirm the precision and accuracy of the predictive model used, which includes major soil and reinforcement factors such as interface friction, geogrid tensile strength, and layer placement. Comparative evaluation against nine other studies highlights the efficiency of the reinforcement strategy as presented, which not only better conventional single-layer approaches, tire-reinforced composites, and even lime-treated hybrid systems but is superior to them. Geogrid application not only improves load transfer but also develops a moisture barrier under the footing, in addition to its longer-term durability.

For further research, it is recommended to scale up the study to field-scale experiments. Full-scale models (e.g., 1 m x 1 m plate) under the same loading conditions as building columns or pavement slabs need to be investigated. Long-term performance observation over environmental conditions such as seasonal variation in groundwater table or surface run-off will provide useful information towards the durability of geogrid materials in other soil chemistries and climate regimes. Chemical degradation, UV weathering, and thermal effects should be avoided over extended periods of service. Green engineering principles should also consider using sustainable or biodegradable geogrid products.

## 6. Declarations

### 6.1. Author Contributions

Conceptualization, R.S.T. and B.M.S.; methodology, R.S.T.; software, R.S.T.; validation, R.S.T. and B.M.S.; formal analysis, R.S.T.; investigation, R.S.T.; resources, R.S.T.; data curation, R.S.T.; writing—original draft preparation, R.S.T.; writing—review and editing, R.S.T.; visualization, R.S.T.; supervision, R.S.T. and B.M.S.; project administration, R.S.T.; funding acquisition, R.S.T. and B.M.S. All authors have read and agreed to the published version of the manuscript.

### 6.2. Data Availability Statement

The data presented in this study are available in the article.

### 6.3. Funding

The authors received no financial support for the research, authorship, and/or publication of this article.

### 6.4. Conflicts of Interest

The authors declare no conflict of interest.

## 7. References

- [1] Abdel-Rahman, M. M. (2020). Review of Soil Improvement Techniques. *Advancements in Geotechnical Engineering*, 175–199, Springer, Cham, Switzerland. doi:10.1007/978-3-030-62908-3\_14.
- [2] Raut, Z. P., & Verma, M. P. (2024). Comprehensive Review of Soil Stabilization through Reinforcement Methods in Civil Engineering. *International Journal of Innovative Research in Technology and Science*, 12(2), 520-530.
- [3] Kumar, S., & Singh, S. K. (2023). Subgrade soil stabilization using geosynthetics: A critical review. *Materials Today: Proceedings*. doi:10.1016/j.matpr.2023.04.266.
- [4] Afrin, H. (2017). A Review on Different Types Soil Stabilization Techniques. *International Journal of Transportation Engineering and Technology*, 3(2), 19. doi:10.11648/j.ijtet.20170302.12.
- [5] Wang, Z., Zhu, J., & Ma, T. (2024). Review on monitoring of pavement subgrade settlement: Influencing factor, measurement and advancement. *Measurement: Journal of the International Measurement Confederation*, 237. doi:10.1016/j.measurement.2024.115225.
- [6] Wang, X., Cheng, C., Zhang, J., Ma, G., Li, J., & Jin, J. (2023). Real-time monitoring and quality assessment of subgrade compaction: key factors and ANN model. *Acta Geotechnica*, 18(6), 3349–3366. doi:10.1007/s11440-022-01769-1.
- [7] Jeon, H.-Y. (2019). Polymeric Synthetic Fabrics to Improve Stability of Ground Structure in Civil Engineering Circumstance. In *Engineered Fabrics*. IntechOpen. doi:10.5772/intechopen.81246.

- [8] Hasheminezhad, A. (2024). Sustainability in geotechnical engineering: Contributions from recycled plastics. Master Thesis, Iowa State University, Ames, United States.
- [9] Chatrabhuj, & Meshram, K. (2024). Use of geosynthetic materials as soil reinforcement: an alternative eco-friendly construction material. *Discover Civil Engineering*, 1(1), 41. doi:10.1007/s44290-024-00050-6.
- [10] Tanasă, F., Nechifor, M., Ignat, M. E., & Teacă, C. A. (2022). Geotextiles—A Versatile Tool for Environmental Sensitive Applications in Geotechnical Engineering. *Textiles*, 2(2), 189–208. doi:10.3390/textiles2020011.
- [11] Prasad, V. V. B., Ishwarya, M. V. S., Jayakrishnan, P., Sathyan, D., & Muthukumar, S. (2023). Applications of natural geotextile in geotechnical engineering. *Materials Today: Proceedings*, 366. doi:10.1016/j.matpr.2023.05.366.
- [12] Abdulrazzak, I. A. (2025). Studying and Assessment of Water Quality of Euphrates River in Iraq. *Al-Iraqia Journal for Scientific Engineering Research*, 4(1), 39-45.
- [13] Jones, A. C. (2024). Field Evaluation of Geogrid-Reinforced Pavement Systems Over Soft Subgrades. Master Thesis, The University of Utah, Salt Lake City, United States.
- [14] Paige-Green, P., & Verhaeghe, B. M. (2018). Making Africa's roads more resilient to climate change. *ResearchSpace, CSIR*, 1-11.
- [15] Marion, J. L., Arredondo, J., & Meadema, F. (2022). Assessing the condition and sustainability of the trail system at Tallgrass Prairie National Preserve. U.S. Geological Survey, Reston, United States.
- [16] Garcia Delgado, I. E. (2015). Use of Geotextiles with Enhanced Lateral Drainage in roads over expansive clays. PhD Thesis, University of Texas at Austin, Austin, United States.
- [17] Abduljaleel, Y. W. (2025). High-Temperature Effects on Punching Shear Performance of Hybrid Reinforced Concrete Slabs. *Al-Iraqia Journal for Scientific Engineering Research*, 4(1), 46-60.
- [18] Li, T. T., Zhou, X., Wang, Z., Fan, Y., Zhang, X., Lou, C. W., & Lin, J. H. (2022). A study on design and properties of woven-nonwoven multi-layered hybrid geotextiles. *Journal of Industrial Textiles*, 51(1), 640S-658S. doi:10.1177/1528083720964703.
- [19] ivek (2024). Degradability of Woven/Non-woven Fabric Polymer Laminates. *Innovations in Woven and Non-woven Fabrics Based Laminated Composites*. Composites Science and Technology, Springer, Singapore. doi:10.1007/978-981-97-7937-6\_14.
- [20] Kumar, S. (2023). Study of Geosynthetics and use of Non-Woven Green Geocomposite Blanket for Erosion Control and Slope Protection for Embankment. *International Research Journal of Engineering and Technology*, 10(4), 1657-1663.
- [21] Ahmad, H. (2022). Sustainability effect of geogrid reinforced tire-shred sand mixtures on the load pressure-settlement response of shallow footing. *Heliyon*, 8(11). doi:10.1016/j.heliyon.2022.e11743.
- [22] Dwivedi, N., Chauhan, V. B., Kumar, A., Jaiswal, S., & Singh, T. (2024). Enhancing strip footing bearing capacity on soil slopes with geogrid reinforcement: insights from finite element analysis and machine learning. *Innovative Infrastructure Solutions*, 9(11), 440. doi:10.1007/s41062-024-01769-y.
- [23] Yousuf, S. M., Khan, M. A., Ibrahim, S. M., Ahmad, F., & Samui, P. (2024). Experimental and Computational Analysis of lime-treated geogrid-reinforced Silty Sand Beneath Circular Footings. *Iranian Journal of Science and Technology - Transactions of Civil Engineering*, 1–22. doi:10.1007/s40996-024-01551-1.
- [24] Mudgal, A., Sarkar, R., Kumar Shrivastava, A., Mishra, U., Meshram, K., Imam, A., & Singh, A. N. (2025). Settlement in geosynthetic reinforced square footing over cohesive soil. *International Journal of Geotechnical Engineering*, 19(4), 202–212. doi:10.1080/19386362.2025.2458497.
- [25] Kumar, S., & Roy, L. B. (2022). Rainfall Induced Geotextile Reinforced Model Slope Embankment Subjected to Surcharge Loading: A Review Study. *Archives of Computational Methods in Engineering*, 29(5), 3203–3221. doi:10.1007/s11831-021-09688-2.
- [26] Saad, A. H., Nahazanan, H., Yusuf, B., Toha, S. F., Alnuaim, A., El-Mouchi, A., Elseknidy, M., & Mohammed, A. A. (2023). A Systematic Review of Machine Learning Techniques and Applications in Soil Improvement Using Green Materials. *Sustainability (Switzerland)*, 15(12), 9738. doi:10.3390/su15129738.
- [27] Sills, G. C. (1975). Some conditions under which Biot's equations of consolidation reduce to Terzaghi's equation. *Geotechnique*, 25(1), 129–132. doi:10.1680/geot.1975.25.1.129.